P. OSTROM

Division of Physical Metallurgy,
Royal Institute of Technology,
Stockholm, Sweden

R. LAGNEBORG

Swedish Institute of Metals
Research, Stockholm, Sweden

A Recovery-Athermal Glide Creep Model

A theoretical recovery-creep model which takes the distribution of dislocation link lengths into account is developed. The recovery process is assumed to be climb controlled. The glide process is critically discussed and is found to be an athermal process. As a consequence of the athermal glide process the model predicts a time interval with the strain rate equal to zero after a small stress reduction. The model is able to simulate the strain-time behavior both in the primary and secondary stage and to simulate the distribution of dislocation link lengths. The stress dependence of the model is evaluated.

Introduction

Based on a description of the dislocation structure as a network consisting of dislocation links in a spectrum of sizes, models have recently been presented for high temperature creep as well as plastic flow at ambient temperatures [1, 2].[1] The creep model suffered from certain inadequacies. In particular, experimental work subsequent to these publications has shown quite unequivocally that the effective stress for dislocation glide is essentially zero during high temperature creep. Hence this implies that glide is an athermal process during creep conditions. The assumption made in this model and in a number of other investigations that the effective stress takes a substantial proportion of the applied stress is therefore erroneous.

The aim of the present work is to develop a dislocation model for high temperature creep based on the ideas and concepts introduced in the model mentioned above. The effort will be to overcome the shortcomings of this model. Particularly it will be developed to be consistent with the finding that the glide process is athermal.

General Ideas About Creep

During plastic deformation the dislocations can often be assumed to exist in a complex three-dimensional network built up by dislocation links joined in nodes. In particular, such a description of the dislocation structure appears to be valid during creep deformation [3]. The dislocation links are known to be of quite varying lengths [4].

In the temperature range of creep ($T > 0.5\ T_m$) the dislocation network recovers. The average dislocation mesh increases its size by means of climb, and the dislocation density decreases [4]. Dislocation links which have increased their lengths sufficiently will be able to surmount the obstacles which oppose glide. The links start to glide, expand into loops, and are eventually arrested by the surrounding network. This process provides strain and an increase of the dislocation density. The glide and recovery process will repeat themselves. Since the glide process is directly dependent on the recovery event and since they have opposite effect on the dislocation production, they will tend to balance each other.

To describe the creep mechanism accurately we must know if the obstacles opposing glide are of thermal or athermal type. These two cases can be sorted out by studying the variation of the flow stress (at a certain plastic strain) with temperature. Results from experiments with pure single-crystals of copper and aluminum show that the flow stress compensated for the temperature dependence of the shear modulus falls with increasing temperature up to about room temperature and is constant from this temperature to about 0.4 T_m. For Cu the compensated flow stress is constant between 250K and 470K. The strain rates of these experiments are slightly higher than the initial strain-rate in the creep experiment which will be simulated by this model [5, 6]. This means that below 250K the obstacles controlling glide can be surmounted by means of stress assisted thermal activation. Examples of such obstacles are the creation of jogs in dislocations gliding through a forest of dislocations and the thermal creation of point defects at jogs in moving screw dislocations. Evidently the obstacles which can be surmounted by means of thermal activation become insignificant in the vicinity of room temperature . The fact that the temperature compensated flow stress is constant for copper in the temperature range 250K to 470K implies that the obstacles controlling glide are athermal in this range. These athermal obstacles are generally assumed to be the attractive junctions and/or the general long-range stress fields of the network. They are associated with long-range elastic fields and the energy needed for a dislocation to surmount any of them is several hundred electron volts. Consequently the attractive junctions and the long range stress fields will remain athermal at much higher temperatures, i.e., in the temperature range of creep. Because of this and because it is bascially impossible for a new type of thermally activatable obstacle to appear as the controlling factor of the glide process beyond an

[1]Numbers in brackets designate References at end of paper.

Contributed by the Materials Division of THE AMERICAN SOCIETY OF MECHANICAL ENGINEERS and presented at the Conference on Micromechanical Modelling of Flow and Fracture, Troy, N. Y., June 23–25, 1975. Manuscript received by the Materials Division, December 9, 1975. Paper No. 75-Mat-1.

athermally controlled range it has to be concluded that the glide in the creep range is an athermal event and is controlled by the overcoming of the attractive junctions and/or the long-range stress fields of the dislocation network.

A consequence of the assumptions in the previous section is that the time it will take a dislocation link to grow long enough to surmount its obstacle must be much longer than the time for the movement from one athermal obstacle to the next. This implies that at a certain moment the creep process can be characterized by a three-dimensional network in which practically all dislocation links are at rest. Many dislocation links, especially the shorter ones, will probably never surmount their obstacles.

The shear stress needed for a dislocation link to surmount an athermal obstacle is given by the equation

$$\tau_i = \alpha G b/l \tag{1}$$

where α is the strength of the obstacle, G is the shear modulus, b is the burgers vector, and l is the length of the dislocation link. Equation (1) is appropriate for attractive junctions and/or long-range stress fields. The value of α depends on the special circumstances. Different links will in general have different values of α. The applied shear stress is τ_a. If the dislocation link is arrested by the obstacle this implies that $\tau_a < \tau_i$. The local effective stress for glide can now be defined as

$$\tau_e = \tau_a - \tau_i \tag{2}$$

For all arrested links τ_e is negative. For a moving link τ_e is positive. According to the earlier reasoning that virtually all links are arrested in the network an average value of all the local effective stresses for glide must be negative.

In this model the recovery process is considered to be a climb controlled shrinkage of small meshes in the network and a growth of the large ones. This will be discussed in detail later. For a dislocation link whose length is continually increasing by recovery, the local effective stress for glide, τ_e, will continually increase its value. When τ_e reaches zero the link surmounts the obstacle, moves quickly and is arrested at obstacles where τ_e is less than zero. The rate at which the dislocation links surmount their obstacles, and consequently the strain rate, is according to this reasoning entirely determined by the recovery process.

The results of the earlier discussion can be used to predict what will happen if we make a small stress reduction, $\Delta\tau_a$, in a creep experiment. Instantaneously before the stress reduction virtually all dislocation links are arrested in the network. These links will therefore determine the main behavior after the stress reduction. Those links which are moving instantaneously before the stress reduction are such a small fraction of the total number of links that they will not be able to alter the main behavior after the stress reduction. For the arrested links the range of the local effective stresses for glide is $\tau_e < 0$ instantaneously before the stress reduction. The links with τ_e equal to zero will, if by means of recovery they increase their lengths infinitesimally, surmount their obstacles. According to equation (2) the effect of the stress reduction is to subtract $\Delta\tau_a$ from all the τ_e's. Instantaneously after the stress reduction none of the links will therefore be able to surmount their obstacles. After a certain time some of the links have by means of recovery increased their lengths enough to make their τ_e's equal to zero. During this time interval the strain rate will virtually cease. The length of the time inverval is determined by the recovery process and it should be longer the larger the stress reduction is. These predictions of the model are experimentally confirmed by stress reduction experiments [7, 8].

A Specific Model

The Physical Background. The general ideas about creep in the previous part are not dependent on any specific structural feature of the dislocation network or on any special type of obstacle opposing glide as long as the obstacles are athermal. For simplicity we will in this specific model make some assumptions about the physical background.

The subgrain formation is typical for high-temperature creep. In the model presented below no special allowance is made for subgrain formation and it is therefore strictly applicable only in the regions where subgrains are absent. Some materials do not exhibit subgrain formation until late in the secondary stage [3, 9, 10]. It has therefore been suitable to use one of these materials, a 20 percent Cr-35 percent Ni steel, to test the model.

The distribution of link sizes in the dislocation network will in accordance with earlier works [1, 2, 4] be described by a frequency function $\phi(l)$. The number of links per unit volume with lengths shorter than l_0 is equal to $N(l_0)$

$$N(l_0) = \int_0^{l_0} \phi(l)dl \tag{3}$$

This means that the number of links in the small interval (l, $l + \Delta l$) is about equal to $\phi(l)\cdot\Delta l$. By means of the frequency function the total dislocation density can now be expressed as

$$\rho(t) = \int_0^{\infty} l\cdot\phi(l, t)dl \tag{4}$$

where the time dependence is included.

We assume that the dislocation links in the network are joined in attractive junctions and that the athermal obstacles of the glide process correspond to the breakage of attractive junctions. The strength of an attractive junction depends on the character of the joining dislocations and the geometry of the junction and it can be of quite varying size [11]. It is possible to compare the calculated values of the strengths of the attractive junctions with the values of the strengths of the obstacles in the real network. If we examine equation (1) it turns out that the strength of an obstacle which has arrested a link of length l must be at least $\alpha = \tau_a l/Gb$, i.e., $\alpha_{max} = \tau_a l_{max}/Gb$. The applied shear stress, τ_a, is supposed to equal the applied tensile stress divided by the Taylor factor which equals 3.1 for fcc metals. In a recent creep study the longest links of the network were estimated to be about 10^{-6} m at a creep stress of 108 MN/m^2. The resulting value of α_{max}, using $G = 6.10^4$ MN/m^2 and $b = 2.5\cdot10^{-10}$ m, is 2.3. This means that the strengths of the obstacles in the network are all less than about 2.3. This is in good agreement with the calculated values for attractive junctions [11].

In the dislocation network the creep process may be considered to take place by the following three subprocesses.

1 By climb controlled shrinkage of small meshes and growth of large meshes the average mesh size will grow.
2 Under the action of the applied stress the growing dislocation links will, when they have gained an appropriate length, be released by the breakage of junctions in the network.
3 The released links expand to loops by glide. The expanding loops will be blocked by adjacent parts of the network.

The subprocess (1) is a recovery process and produces always a decrease in the dislocation density. The subprocesses (2) and (3) are together a strain hardening process which always produces an increase in the dislocation density.

Formulation of the Model. We will now describe the three subprocesses, one at a time, in a mathematical form.

1 The treatment of the recovery process is the same as in an earlier work [1]. Direct measurements of the distribution of mesh sizes [4, 9] have shown that the recovery of the dislocation structure during creep conditions occurs by a shrinkage and eventual disappearance of the small meshes and a growth of the large meshes, the net result of which is a growth of the meshes of the network. This process requires that the dislocation links of the meshes are in general free to move in any crystal-plane and not only in the slip planes. During high temperature con-

ditions the climb process provides this freedom and therefore it is generally assumed that the recovery is climb-controlled. The driving force of the process is the self-energy or the line-tension of the dislocations. Hence, we notice that there is quite a close resemblance between the growth process of the dislocation meshes and grain growth. Therefore, in accordance with the theory for grain growth [12] we will assume that the individual meshes will change their radius (R) with time as

$$\frac{dR}{dt} = \beta M T \left(\frac{1}{R_{cr}} - \frac{1}{R} \right) \tag{5}$$

β is a numerical constant which is expected to equal 0.5–1.0 from the theory of grain growth and therefore we put $\beta = 1$. M is the mobility of the climbing dislocations. T is the dislocation line tension. We use $T = Gb^2/2$. $T(1/R_{cr} - 1/R)$ is the driving force for the growth or shrinkage. R_{cr} is the critical size above which the meshes grow and below which they shrink. The mesh growth/grain growth analogy fails on one point. The dislocation links interact elastically over long ranges, whereas a corresponding long range interaction is negligible for grain boundaries. However, it appears that this difference does not affect the analogy seriously, since experiments have shown that the variation of mesh size with time, due to recovery, follows closely the relation for the growth law of average grain size ($\bar{R}$), which can be derived from equation (5) ($d\bar{R}/dt \propto M/\bar{R}$) [4]. It may be that the long range elastic interaction between the links on the average cancels out, and therefore has no major influence on the overall process.

The change of mesh sizes according to equation (5) results in an exchange of links between neighboring size classes. The change of the number of links in a size class (R, $R + \Delta R$) during the time interval (t, $t + \Delta t$) may be written as

$$\Delta\phi(R, t) \cdot \Delta R = -\left(\phi(R + \Delta R) \cdot \frac{dR}{dt}(R + \Delta R) - \phi(R) \cdot \frac{dR}{dt}(R) \right) \cdot \Delta t \tag{6}$$

This relation gives the differential equation

$$\frac{\partial \phi(R, t)}{\partial t} = -\frac{\partial}{\partial R}\left(\phi(R, t) \cdot \frac{dR}{dt} \right) \tag{7}$$

which thus describes the change of ϕ due to the continuous mesh growth. The mesh radius, R, will only differ from the link length of the mesh, l, by a constant factor, not very far from one. We simply assume, therefore, that R equals l. By substitution of equation (5) into equation (7) we obtain the final expression for the change of ϕ due to recovery.

$$\frac{\partial \phi(l, t)}{\partial t}\Big/_{r} = -MT\left(\frac{1}{l_{cr}(t)} - \frac{1}{l} \right) \cdot \frac{\partial \phi(l, t)}{\partial l} - MT \cdot \frac{1}{l^2} \cdot \phi(l, t) \tag{8}$$

The remaining problem is to calculate $l_{cr}(t)$. This will be discussed later.

2 The implication of the physical description of creep given above is that only the growing links in the recovery process will be able to break their junctions and glide, thereby adding strain to the creep. Hence, according to the mathematical formulation of the recovery, equation (5), only links larger than l_{cr} will have a chance to participate in the glide process. When the links of this category have gained sufficient length to satisfy equation (1), $\tau_a = \alpha Gb/l$, glide occurs.

If the attractive junctions could be adequately described by one single strength (α) the creep rate should be directly given by the flux of dislocation links caused by the recovery process passing through the link size $\alpha Gb/\tau_a$. However, as already pointed out the junctions may occur in a spectrum of strengths. This means that in a loaded specimen, like a creep specimen, the attractive junction opposing a particular link of length l will have a strength equal to or larger than $\alpha = \tau_a l/Gb$. Links opposed by weaker junctions will of course never be formed. There will always be one type of junction which has the largest possible strength, α_{max}, and this will correspond to the maximum link length existing in the dislocation network through the relationship $l_{max} = \alpha_{max} Gb/\tau_a$. Evidently the spectrum of junction strengths for a particular link length will be larger the smaller the link size is. For the extremes of the growing links, l_{cr} and l_{max}, the range of strength will shrink from $\alpha_{max} - \alpha_{cr}$ to a single value α_{max}. As a consequence of this it will be only a small fraction of all the links with lengths close to l_{cr} that will be able to break free from their obstacles by an infinitesimal recovery growth. The remaining part needs to grow more. The stronger the junction is the more length must the link gain before it can break free. Close to l_{max}, on the other hand, all the opposing junctions will have strengths close to α_{max} and accordingly the majority of the links can here surmount their obstacles after an infinitesimal growth. These effects are demonstrated in Fig. 1(a) which shows that the relative number of links contributing to the creep process at any particular time increases as l increases from l_{cr} to l_{max}. However, if this idea is pursued in detail it turns out that the model produces a steadily increasing creep rate, hence indicating that the picture of the glide process in Fig. 1(a) is oversimplified. Apparently the number of dislocation links producing glide is drastically overestimated by the idea sketched in Fig. 1(a) as l_{cr} decreases during the creep process. We believe that the main reason for this is that during recovery not only do the link lengths increase but so do also their strengths. During the recovery process the dislocations will arrange themselves in low energy positions and as a consequence the junctions will tend to be stronger. For the rather small growth rates of links close to l_{cr} this probably means that the increase of α overrules the increase of l and that the links in this size range will never break free from their junctions. Whereas the decrease of l_{cr} during creep will tend to enlarge the region of links contributing to glide in Fig. 1(a) this effect will tend to shrink it. As a very simple approximation of this complex situation we will assume that a constant fraction of the existing dislocation links will participate in the glide process above a certain link size $\bar{l}$ as demonstrated in Fig. 1(b). It is quite possible that $\bar{l}$ undergoes a variation during primary creep and reaches a constant value only in the secondary stage. Lacking information of the details of this complex situation we will simply assume it to be constant throughout a creep test. Its depencence of stress is assumed to obey equation (1), $\bar{l} = \bar{\alpha} Gb/\tau_a$. The change of the frequency function due to such a glide process can be expressed mathematically as

$$\frac{\partial \phi(l, t)}{\partial t} = -B \cdot \phi(l, t) \cdot H(l - \bar{l}) \tag{9}$$

$H(l)$ is defined by

$$H(l) = \begin{cases} 0 \text{ if } l < 0 \\ 1 \text{ if } l \geqslant 0 \end{cases} \tag{10}$$

B is a constant which will be related to the rate of the recovery process close to $l = \bar{l}$ and will therefore be expected to be quite strongly temperature dependent.

3 When a link has been released by the breakage of a junction it expands into a loop until it is arrested by the adjacent network. In Fig. 2 we have sketched a network and a loop which has been arrested in it. The figure shows that for each link which is hit three new links are formed. These three new links have in general different lengths but for simplicity we make the following assumption. When a link of length $l/k(t)$ ($k(t) < 1$) is hit

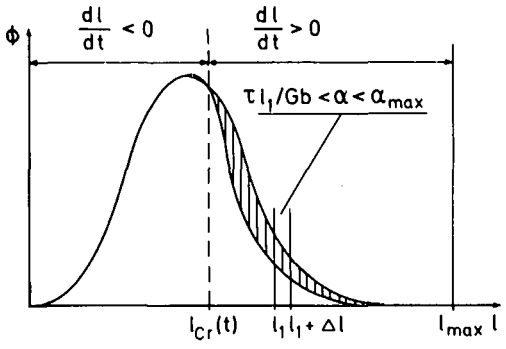

Fig. 1(a)

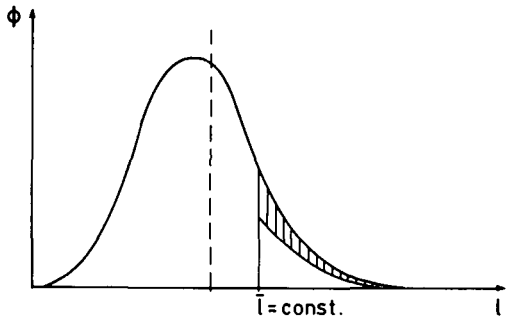

Fig. 1(b)

Fig. 1 The shaded areas correspond to the links which will break their junctions during the time interval $(t, t + \Delta t)$ due to the recovery process. In (a) the behavior is shown if the strengths of the junctions are not changed by the recovery process and in (b) the behavior is shown due to the approximation in this model.

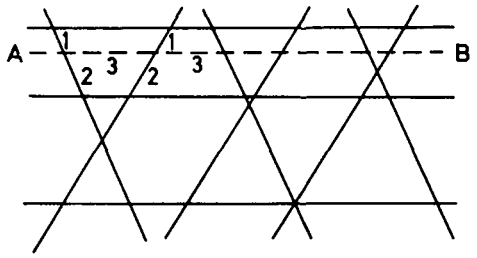

Fig. 2 A dislocation loop AB is arrested in the dislocation network. The figure shows schematically that for each dislocation link which is hit (1-2) three new links (1, 2, 3) are created.

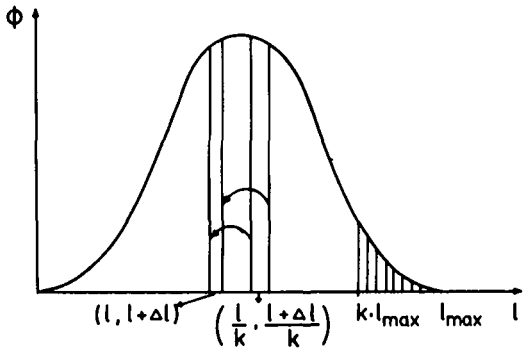

Fig. 3 When a dislocation link in the interval $(l/k, (l + \Delta l)/k)$ is hit by an expanding loop three new dislocation links in the interval $(l, l+\Delta l)$ are created. A drawback of this simplification is that there will be no supply of new links due to the strain hardening process in the interval (kl_{max}, l_{max}).

the three links will have a length of l, which we may associate with the mean of their actual lengths. The assumption that $k(t) < 1$ is due to the experimental fact that the dislocation density increases during a strain-hardening process, i.e., the mean link length decreases.

We make one more assumption. The probability that a link of length l will be hit by an expanding loop during the time interval $(t, t + \Delta t)$ is equal to $C(t) \cdot l \cdot \Delta t$. $C(t)$ depends for instance on the strain rate.

We are now able to express the net increase in the number of links in the interval $(l, l + \Delta l)$ during the time interval $(t, t + \Delta t)$.

$$\Delta\phi(l, t) \cdot \Delta l = 3 \cdot C \cdot (l/k) \cdot \Delta t \cdot \phi(l/k, t) \cdot (\Delta l/k) - C \cdot l \cdot \Delta t \cdot \phi(l, t) \cdot \Delta l \quad (11)$$

hence

$$\frac{\partial\phi(l, t)}{\partial t} = C(t) \cdot l \cdot \left(\frac{3}{(k(t))^2} \cdot \phi\left(\frac{l}{k(t)}, t \right) - \phi(l, t) \right) \quad (12)$$

The first term in equation (11) expresses the supply of new links in $(l, l + \Delta l)$ due to links which are hit in the interval $(l/k, (l + \Delta l/k))$. The second term expresses the number of links which are hit in the interval $(l, l + \Delta l)$. This formulation has a drawback which is illustrated in Fig. 3. The function $k(t)$ is assumed to be a mean-value in the whole network and is therefore independent of l. As a consequence there will be no supply of new links in the interval $(k \cdot l_{max}, l_{max})$. According to the numerical calculations the value k is about 0.75. However, this drawback does not influence the results of the calculations in a serious way. The final expression for the change of $\phi(l, t)$ due to strain-hardening can be written as

$$\left.\frac{\partial\phi(l, t)}{\partial t}\right|_{sh} = -B \cdot \phi(l, t) \cdot H(l - \bar{l}) + C(t) \cdot l \cdot \left(\frac{3}{(k(t))^2} \cdot \phi\left(\frac{l}{k(t)}, t \right) - \phi(l, t) \right) \quad (13)$$

To determine the functions $C(t)$ and $k(t)$ we have to make some assumptions. The mean free path of motion for the dislocation links from their release at an obstacle to their arrest at the next obstacle will be designated λ. We assume

$$\lambda(t) = L \cdot (\rho(t))^{-1/2} \quad (14)$$

where L is a constant. The expansion of dislocation loops gives rise to both an increase in strain and an increase in dislocation density. For the relation between these two quantities we assume

$$\left.\frac{d\rho}{dt}\right|_{sh} = \frac{1}{b\lambda}\frac{d\gamma}{dt} = \frac{1}{bL} \cdot \rho^{1/2} \cdot \frac{d\gamma}{dt} \quad (15)$$

where γ is the shear strain.

In a three-dimensional network where the geometry does not change with time the condition of constant volume is expressed by [12]

$$\int_0^\infty l^3\phi(l, t)dl = \text{constant} \quad (16)$$

hence

$$\int_0^\infty l^3 \frac{\partial\phi}{\partial t}\, dl = 0 \quad (17)$$

This condition is supported by experiments [4]. We assume that the condition of constant volume must apply independently of the strain hardening process, equation (13), and to the recovery process, equation (8). This means

$$\int_0^\infty l^3 \left.\frac{\partial \phi}{dt}\right/_{sh} dl = \int_0^\infty l^3 \left.\frac{\partial \phi}{dt}\right/_{r} dl = 0 \qquad (18)$$

This condition of constant volume together with the relation between the strain and the dislocation density, equation (15), determine the functions $C(t)$ and $k(t)$ in the strain hardening process. For the recovery process the condition of constant volume determines the value of $l_{cr}(t)$.

$$l_{cr}(t) = \frac{\int_0^\infty l^2 \phi dl}{\int_0^\infty l \phi dl} \qquad (19)$$

The total change in the frequency function $\phi(l, t)$ can now be expressed as the sum of the strain hardening process and the recovery process, i.e., the sum of equation (13) and equation (8).

$$\frac{\partial \phi(l, t)}{\partial t} = -B \cdot \phi(l, t) \cdot H(l - \bar{l}) + C(t) \cdot l \cdot \left(\frac{3}{(k(t))^2} \cdot \phi\left(\frac{l}{k(t)}, t \right) - \phi(l, t) \right) - MT \cdot \left(\frac{1}{l_{cr}(t)} - \frac{1}{l} \right) \cdot \frac{\partial \phi(l, t)}{\partial l} - MT \cdot \frac{1}{l^2} \cdot \phi(l,t) \qquad (20)$$

The remaining quantity to be determined is the strain rate. The number of links per unit volume which break their junctions per unit time are

$$\frac{dN}{dt} = \int_{\bar{l}}^\infty B \cdot \phi(l, t) dl \qquad (21)$$

If A is the average area a released link passes over until it is pinned, the shear strain rate can be expressed as

$$\frac{d\gamma}{dt} = bA \frac{dN}{dt} \qquad (22)$$

By making use of the two ways of expressing the strain created by the dislocation loops per unit volume, $\Delta\gamma = bA\Delta N$ and $\Delta\gamma = b\lambda\Delta\rho$, it is apparent that there always exists a relation between A and λ. However, this depends on the geometry of the loop. If we for simplicity assume that the loop is circular it is readily shown that the radius of the loop equals 2λ, i.e., $A = 4\pi\lambda^2 = 4\pi L^2/\rho$. The expression for the strain rate may now be written as

$$\frac{d\gamma}{dt} = \frac{4\pi b L^2}{\rho} \cdot \int_{\bar{l}}^\infty B \cdot \phi(l, t) dl \qquad (23)$$

The normal strain, ϵ, can be expressed as $\epsilon = \gamma/m$, where m is the Taylor factor. For fcc metals m is equal to 3.1. The equations determining the creep process can now be summarized.

$$\frac{\partial \phi(l, t)}{\partial t} = -B \cdot \phi(l, t) \cdot H(l - \bar{l}) + C(t) \cdot l \cdot \left(\frac{3}{(k(t))^2} \cdot \phi\left(\frac{l}{k(t)}, t \right) - \phi(l, t) \right) - MT \cdot \left(\frac{1}{l_{cr}(t)} - \frac{1}{l} \right) \cdot \frac{\partial \phi(l, t)}{\partial l} - MT \cdot \frac{1}{l^2} \cdot \phi(l, t) \qquad (24a)$$

$$\frac{d\epsilon}{dt} = \frac{4\pi b L^2}{3.1 \cdot \rho(t)} \cdot \int_{\bar{l}}^\infty B \cdot \phi(l, t) dl \qquad (24b)$$

$$\left.\frac{d\rho}{dt}\right/_{sh} = \frac{3.1}{bL} \cdot (\rho(t))^{1/2} \cdot \frac{d\epsilon}{dt} \qquad (24c)$$

$$\int_0^\infty l^3 \frac{\partial \phi(l, t)}{\partial t} dl = 0 \qquad (24d)$$

The value of B is determined by equation (24b) if we make use of the experimentally determined initial strain rate and initial ϕ-function. The remaining three parameters $\bar{l}$, L, and M are used in the simulations to obtain good fits between the calculated and experimental creep curves and the calculated and experimental steady state ϕ-functions. An important feature of the model is that all the quantities in the model, constants and functions, have a definite physical meaning.

Simulation of Creep Deformation

Determination of the Parameters of the Model. The objective of the numerical computations has been to simulate the creep deformation in the primary stage and the secondary stage in a 20 percent Cr-35 percent Ni steel. This material was chosen because good measurements of the variation of the creep strain and the frequency function ϕ with time were available and its dislocation structure is fairly homogeneous in the primary and the early secondary state [4, 9]. To determine the parameters of the model we have chosen to simulate a creep experiment performed at 973K and at the tensile stress 108 MN/m^2.

The calculations were started up from the experimentally determined frequency function $\phi_0(l)$ and initial strain rate $\dot{\epsilon}_0 \cdot \phi_0$ corresponds to the dislocation network which exists after the loading and the instantaneous strain. ϕ_0 is very well approximated by the analytical function $3.2 \cdot 10^{44} l^3 \exp(-8.0 \cdot 10^{18} l^3) \mathrm{m}^{-4}$. This distribution corresponds to an initial dislocation density of $3.0 \cdot 10^{12} \mathrm{m}^{-2}$. The initial strain rate was $1.45 \cdot 10^{-5}$ s^{-1}.

In order to solve equation (24) numerically an implicit difference method was used. The accuracy of the results has been checked by varying the space step, δl, and the time step, δt.

By varying $\bar{l}$, L, and M good fits between the calculated and experimental creep curves (Fig. 4) and between the calculated and experimental steady state ϕ-functions (Fig. 5) are obtained. The values for the good fits are $\bar{l} = 2.6 \cdot 10^{-7}$m, $L = 0.65$, and $M = 0.13$ m^2/(MN $\cdot$ s). It turned out that for any reasonable value of $\bar{l}$ a good fit between the creep curves is obtainable. The strain of the primary stage is mainly determined by L. Consequently M was used to adjust the strain rate in the secondary stage. To get a good fit between the steady state ϕ-functions at the same time as a good fit between the creep curves was obtained it was necessary to vary $\bar{l}$. The variation with time of the calculated ϕ-functions is shown in Fig. 5. The calculated dislocation density (Fig. 6) increases very fast during the primary stage in correspondence with the fast decrease of the strain rate. Both the dislocation density and the strain rate approach constant values. The same is true for all other quantities. The experimental dislocation density reaches a constant value much later as can be seen in Fig. 6. The function $k(t)$ varies slowly with time from 0.72 to 0.79. This is in accordance with the assumption of a homogeneous network. The function $C(t)$ decreases very fast during the primary stage from $2.8 \cdot 10^5$ to $2.7 \cdot 10^4$ (m $\cdot$ s)$^{-1}$. This means that the probability that a link of length 2.10^{-7} m is hit during one second equals $5.4 \cdot 10^{-3}$ in the secondary stage. This is in accordance with the assumption that almost all links are arrested in the network and only a few are gliding. The function $l_{cr}(t)$ decreases very fast from $5.5 \cdot 10^{-7}$ to $1.7 \cdot 10^{-7}$ m. The value of B is $1.8 \cdot 10^{-2}$ s^{-1}.

A test of the model is to compare the values of $\bar{l}$, L, and M obtained from the numerical simulations with values determined in an independent way. In this model the obstacles are assumed to be the attractive junctions. For a dislocation gliding through

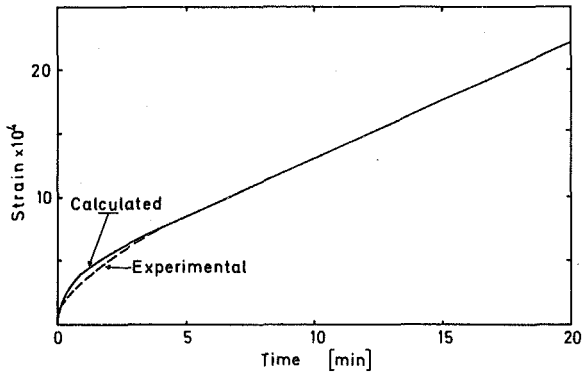

Fig. 4 Calculated and experimental creep curves (108 MN/m²)

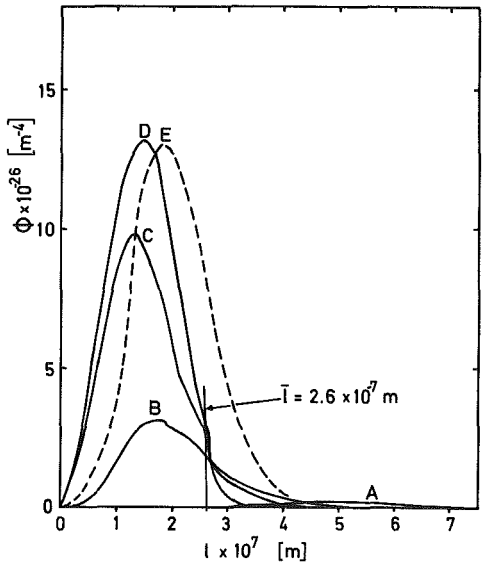

Fig. 5 Calculated and experimental frequency functions (108 MN/m²)
(A) Experimental curve at $t=0$ and initial curve for the calculation
(B, C) Calculated curves at $t=15$ s and $t=45$ s
(D) Calculated steady state curve
(E) Experimental steady state curve

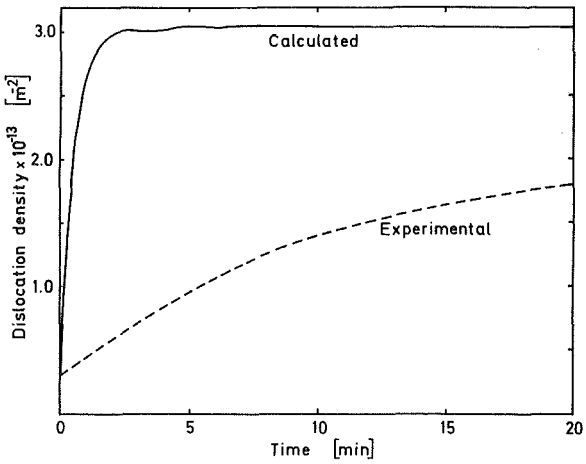

Fig. 6 Calculated and experimental dislocation densities (108 MN/m²)

a forest of dislocations about every second intersection is attractive. Consequently the diameter of an expanded dislocation loop should be about $2 \cdot \rho^{-1/2}$. This estimation is in good agreement with the value of the diameter produced by the model which is equal to $4L\rho^{-1/2} = 2.6 \cdot \rho^{-1/2}$.

The value of $\bar{l}$ corresponds to a value of $\bar{\alpha} = 0.60$ (equation (1)). This value can be compared with the value of α' in the relation

$$\tau_a = \alpha' G b \rho_s^{1/2} \tag{25}$$

The steady state dislocation density, ρ_s, is $3.0 \cdot 10^{13}$ m^{-2} and the corresponding value of α' is 0.43. However, in equation (25) the total dislocation density is used, i.e., not only the long links, and this must necessarily give a smaller value of α' than $\bar{\alpha}$.

The model predicts a strain rate equal to zero instantaneously after an arbitrarily small stress reduction. It is, however, not possible to simulate stress reductions by equation (24). A rough estimate of the length of the time interval with zero strain rate after a small stress reduction in the secondary stage can be made. We calculate the length of this time interval in the secondary stage for links of length $\bar{l}$ and assume that this value is representative. A link of length $\bar{l}$ which instantaneously before the stress reduction was on the verge of breaking its junction must after the stress reduction increase its length before it is able to break its junction again. The required increase in length for a small stress reduction, $\Delta\tau_a$, is given by equation (1)

$$\Delta\bar{l} \simeq \bar{l}\Delta\tau_a/\tau_a \tag{26}$$

The rate of growth of the link is given by equation (5) and for a small stress reduction we assume it to be constant during the small time interval with zero strain rate. The length of the time interval is now given by

$$\Delta t \simeq \Delta\bar{l} / \frac{d\bar{l}}{dt} \simeq \bar{l}\Delta\tau_a/(\tau_a M T(1/l_{cr} - 1/\bar{l})) \tag{27}$$

For a stress reduction of 1 percent this gives $\Delta t = 5.2$ s. An independent value obtained from experiments is $\Delta t = 1.3$ s [8]. Hence, from this we conclude that the M-value obtained from the model is, within a factor of 4, in agreement with independent experiments. In view of the incertainties in the measurement and the calculation (equation (27)) of Δt this must at the present stage be considered satisfactory.

Dependence of the Results on the Initial Values. In a creep model, like the present, one would expect the steady state properties to be independent of the initial state at which creep commences. To test this assumption the initial values ϕ_0 and $\dot{\epsilon}_0$ have been varied. The function ϕ_0 has been approximated by the function $Al^3 \cdot \exp(-Bl^3)$. The constants A and B are determined by the initial dislocation density and the condition of constant volume (equation (16)). A variation of the initial dislocation density from $0.5\rho_0$ to $1.5\rho_0$, where ρ_0 is the experimentally determined value, yields a variation in the steady state creep rate of 5 percent and in the steady state dislocation density of 3 percent. A variation of the initial creep rate from $0.5\dot{\epsilon}_0$ to $1.5\dot{\epsilon}_0$ yields a variation in the steady state creep rate of 12 percent and in the steady state dislocation density of 23 percent. Hence the steady state creep rate and the steady state dislocation density are approximately independent of the initial values.

Dependence of the Steady State Dislocation Density on the Parameters. The relation between the applied stress and the steady state dislocation density in equation (25), $\tau_a = \alpha' G b \rho_s^{1/2}$, is justified on the basis that the glide process is an athermal process. A consequence of this relation is that the steady state dislocation density should be independent of L and M. A variation of L from $0.5L$ to $1.5L$ and of M from $0.5\,M$ to $1.5M$ where L and M are the values obtained from the simulations, yields a variation of $Gb\rho_s^{1/2}$ of only 4 and 8 percent, respectively. Hence the product $Gb\rho_s^{1/2}$ is approximately independent of L and M.

The parameter determining the steady state dislocation density is, as expected, $\bar{l}$ which is related to ρ_s through the relations $\tau_a = \bar{\alpha}Gb/\bar{l}$ and $\tau_a = \alpha' Gb\sqrt{\rho_s}$.

Stress Dependence of the Model. The values obtained for $\bar{\alpha}$, L, and M obtained at the tensile stress 108 MN/m² have been used to simulate two creep experiments at the tensile stress levels 78.5 and 147 MN/m². The experimentally determined values of ρ_0 and $\dot{\epsilon}_0$ were used. It was found that the stress dependence of the steady state creep rate, expressed as the exponent in the usual power law $\dot{\epsilon}_s = A\sigma^n$, is 3.2. The computed stress dependence of the steady state dislocation density proved to follow closely a relationship of the type $\tau_a = \alpha Gb\rho_s^{1/2}$ (cf. Fig. 7). It is instructive to compare these results with a simple recovery creep model which involves the same basic assumptions for the dislocation generation and recovery as the present model [13]. In this, the dislocation structure is assumed to be adequately described by the average quantity, the dislocation density, and no account is taken to the distribution of dislocation link lengths. It predicts a steady state creep rate

$$\dot{\epsilon}_s = 2b\lambda M T \rho_s^2 \tag{28}$$

Inserting $\tau_a = \alpha' Gb\rho_s^{1/2}$ and $\lambda = L \cdot \rho^{-1/2}$ (equation (14)) we arrive at

$$\dot{\epsilon}_s = 2bLMT\left(\frac{\tau_a}{\alpha' Gb}\right)^3 \tag{29}$$

Hence the stress dependence of the creep rate is in rather close accordance between the two models. Furthermore, the dislocation density in the simple model is uniquely determined by $\tau_a = \alpha' Gb\rho_s^{1/2}$. The fact that ρ_s was found to be approximately independent of L and M in the present model proves that also on this point the two models are consistent with each other. These results show that the use of the simple model should in many cases be adequate and sufficient.

The experimentally determined stress dependence of the steady state creep rate is 4.7 [9]. According to our opinion $\bar{\alpha}$ and M are stress independent. Hence L must depend on stress. An increase of L from 0.65 to 0.91 for the stress level 147 MN/m² and a decrease of L from 0.65 to 0.46 for the stress level 78.5 MN/m² yields the stress dependence 4.7 of the steady state creep rate. The corresponding stress dependence of L is $L \propto \sigma^{1.1}$. A possible explanation of this stress dependence is that L depends on cross slip of the gliding dislocations which is a stress-assisted mechanism. Fig. 7 shows that the computed steady state dislocation densities are in reasonable agreement with experimental data. The three creep curves corresponding to the three stress levels are shown in Fig. 8. Since L largely determines the primary creep strain a comparison between computed and experimental primary strains by the application of $L \propto \sigma^{1.1}$ represents an independent test of the model. Below about 120 MN/m² the agreement is quite satisfactory. Above 120 MN/m² the model underestimates the primary creep strain.

Summary and Conclusions

A theoretical recovery creep model has been presented. The model includes the following features.

1 It takes the distribution of link lengths into account.
2 The glide process is assumed to be athermal and as a consequence the effective stress for glide is shown to be negative for the majority of the dislocation links.
3 It predicts a time interval with the strain rate equal to zero after arbitrarily small stress reductions. The length of the time interval is predicted to be longer the larger the stress reduction is.
4 It is able to simulate the strain-time behavior in both the primary and secondary stage and the behavior of the dislocation density and the distribution of dislocation link lengths. The accordance between theory and experiment has been obtained for values of the parameters of the model which are in good agreement with independent theoretical estimates and measurements.
5 The steady state values of the strain rate and the dislocation density are approximately independent of the initial dislocation density and the initial strain rate.
6 The steady state dislocation density follows closely the relation $\tau_a = \alpha' Gb\rho_s^{1/2}$. This relation is justified on the basis that the glide process is an athermal process. It is shown, in accordance with this relation, that the steady state dislocation density is approximately independent of the magnitude of the mean free path of dislocation glide and the mobility of the climbing dislocations.
7 The stress dependence of the steady state creep rate and the steady state dislocation density is in agreement with a simple model for the steady state creep previously proposed by Lagneborg.
8 To obtain the experimentally determined stress dependence of the steady state creep rate it is necessary to assume that the factor L in the relation for the mean free path of dislocation glide, $\lambda = L\rho^{-1/2}$, is stress dependent.

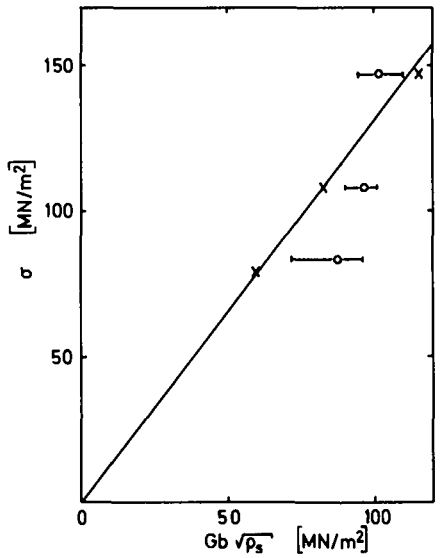

Fig. 7 The tensile stress versus $Gb\rho_s^{1/2}$. ρ_s is the steady state dislocation density. (x) indicates the calculated values and (0) the experimental values.

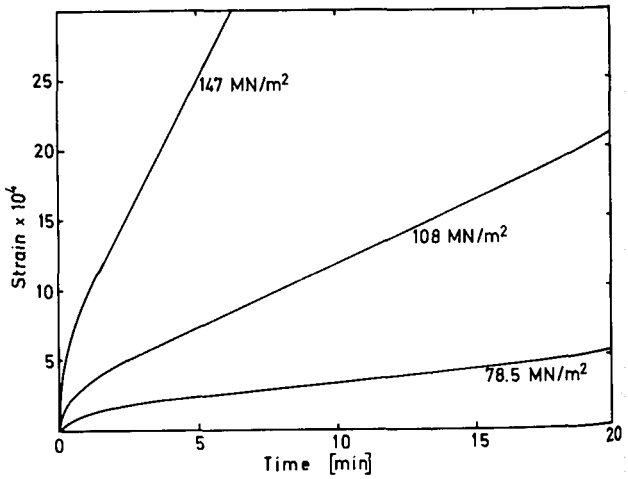

Fig. 8 Calculated creep curves for the tensile stresses 78.5, 108, and 147 MN/m²

Acknowledgment

Financial support by the Swedish Board for Technical Development is gratefully acknowledged.

References

1 Lagneborg, R., Forsen, B.-H., and Wiberg, J., "A Recovery Creep Model Based on Dislocation Distributions," *Proceedings of the Conference on Creep Strength in Steel and High-Temperature Alloys*, Sheffield, Sept. 1972, pp. 1–7.

2 Lagneborg, R., and Forsen, B.-H., "A Model Based on Dislocation Distributions for Work-Hardening and the Density of Mobile and Immobile Dislocations during Plastic Flow," *Acta Metallurgica*, Vol. 21, June 1973, pp. 781–790.

3 Lagneborg, R., "Dislocation Mechanisms in Creep," *International Metallurgical Reviews*, Vol. 17, 1972, pp. 130–146.

4 Oden, A., Lind, E., and Lagneborg, R., "Dislocation Distributions during Creep and Recovery of a 20% Cr-35%-Ni Steel at 700°C," *Proceedings of the Conference on Creep Strength in Steel and High-Temperature Alloys*, Sheffield, Sept. 1972, pp. 60–70.

5 Adams, M. A., and Cottrell, A. H., "Effect of Temperature on the Flow Stress of Work-Hardened Copper Crystals," *The Philosophical Magazine*, Vol. 46, 1955, pp. 1187–1193.

6 Cottrell, A. H., and Stokes, R. J., "Effects of Temperature on the Plastic Properties of Aluminium Crystals," *Proceedings of the Royal Society of London*, Vol. 233, 1955, pp. 17–34.

7 Davies, P. W., et al., "Stress-Change Experiments during High-Temperature Creep of Copper, Iron and Zinc," *Metal Science Journal*, Vol. 7, 1973, pp. 87–92.

8 Bergman, B., "A Note on 'The Strain Transient Dip Test'," TRITA-MAC-0049, June 1974.

9 Modeer, B., "A Study of Creep Deformation of an Austenitic Stainless Steel," Doctoral thesis, The Royal Institute of Technology, Stockholm, Oct. 1974.

10 Evans, W. J., and Wilshire, B., "The High Temperature Creep and Fracture Behavior of 70-30 Alpha-Brass," *Metallurgical Transactions*, Vol. 1, Aug. 1970, pp. 2133–2139.

11 Baird, J. D., and Gale, B., "Attractive Dislocation Intersections and Work Hardening in Metals," *Philosophical Transactions of the Royal Society of London*, Vol. 257, 1965, pp. 553–590.

12 Hillert, M., "On the Theory of Normal and Abnormal Grain Growth," *Acta Metallurgica*, Vol. 13, March 1965, pp. 227–238.

13 Lagneborg, R., "A Modified Recovery-Creep Model and Its Evaluation," *Metal Science Journal*, Vol. 6, 1972, pp. 127–133